Development and assessment of ^{153}Sm-zoledronate complex as a possible bone pain palliative agent

Original Article

Mirsaeed Nikzad[1], Amir Reza Jalilian[2,3], Simindokht Shirvani-Arani[2], Masood Arabieh[2], Saeed Shanesazzadeh[2], Hamid Golchoobian[1]

[1]Department of Inorganic Chemistry, University of Mazandaran, Babolsar, Iran
[2]Nuclear Science and Technology Research Institute (NSTRI), Tehran, Iran
[3]Radioisotope Products and Radiation Technology Section, Department of Nuclear Sciences and Applications, International Atomic Energy Agency (IAEA), Vienna, Austria

(Received 16 August 2016, Revised 31 January 2017, Accepted 2 February 2017)

ABSTRACT

Introduction: In this work, ^{153}Sm-zoledronate (^{153}Sm-ZLD) was studied using computational chemistry methods and prepared for possible use in bone pain palliation therapy.

Methods: The $Sm(ZLD)_2.7H_2O$ complex was synthesized and characterized in solid state using computational chemistry methods followed by ^{153}Sm-ZLD complex production, stablity, hydroxyapatite (HA) tests and also biodictribution studies in animals were studied and used for absorbed dose determination in critical organs.

Results: The $Sm(ZLD)_2.7H_2O$ complex was synthesized and characterized in solid state and computational chemistry methods showed that 1:1, 1:2 and 1:3 complex formation are possible in aqueous solution. ^{153}Sm-ZLD complex was prepared with >99% radiochemical purity (ITLC, HPLC) and specific activity of 4.4 GBq/mmol. It was stable for 24h with >95% binding to HA with accumulation in rat bones and kidneys. Absorbed dose showed kidney and osteogenic tissue as critical organs.

Conclusion: The ^{153}Sm-ZLD complex data were compared to ^{153}Sm-EDTMP and ^{153}Sm-BPAMD.

Key words: ^{153}Sm; Zoledronic acid; Biodistribution; Dosimetry; Bone pain palliation

Iran J Nucl Med 2017;25(2):81-91
Published: July, 2017
http://irjnm.tums.ac.ir

Corresponding author: Dr. Amir Reza Jalilian, Radioisotope Products and Radiation Technology Section, Department of Nuclear Sciences and Applications, International Atomic Energy Agency (IAEA), Vienna International Centre, PO Box 100, 1400, Vienna, Austria. E-mail: a.jalilian@iaea.org

INTRODUCTION

Bisphosphonates are effective drug class for bone pain palliation in patients with different bone complications including malignancies [1] showing strong affinity for calcium phosphates and for hydroxyapatite. The molecules attach preferentially to bone with increased avidity for areas of osteoblastic and osteoclastic activity [2, 3]. Skeletal targeted radiotherapy is performed in patients with metastatic bone pain mostly in patients with metastatic prostate and breast cancers. Several bone-seeking radiopharmaceuticals have been developed for bone pain palliation.

^{153}Sm-EDTMP is the most important radiopharmaceutical used in bone pain palliation [4] and is still used more than other radiopharmaceuticals including ^{89}Sr, ^{186}Re, ^{188}Re and ^{177}Lu radionuclides developed for treatment of painful metastases [5].

Among the therapeutic radionuclides, ^{153}Sm with the favorable radiation characteristics [$t_{1/2}$ = 1.93 d, β^-max = 0.81 MeV (20 %), 0.71 MeV (49 %), 0.64 MeV (30 %) and c = 103 keV (30 %)], is the most promising radionuclide. Many other ^{153}Sm labelled complexes have been developed for palliation therapy of metastasis such as ^{153}Sm-DOTMP [6].

Among various bisphosphonates used in many countries (zoledronate, clodronate, etidronate, pamidronate, alendronate and ibandronate) [7], zoledronic acid (ZLD) is used to reduce the risk of fractures in cancers affecting the bone, most commonly in myeloma and secondary breast/prostate cancers [8].

Radiolabelled ZLD complexes have been reported in the literature for the diagnosis and bone pain palliation studies. For instance, ^{99m}Tc-ZLD was prepared and showed no significant differences compared to ^{99m}Tc-MDP [9], also in continuous effort to develop ^{99m}Tc-based tracers, ^{99m}Tc-labeled butyl-substituted zoledronic acid was developed and demonstrated 24.6 ± 1.65 % ID g^{-1} at 120 min post injection [10]. Nikzad et al. reported the successful development of ^{177}Lu-ZLD with comparable biological performance with ^{177}Lu-EDTMP, however most of direct labelling suffered from minor radionuclide release from the complex *in vivo* [11].

In this work, computational chemistry was used to find the most stable structures Sm/ZLD system of metal/bis phosphonates complexes as reported previously [12] and in the next step ^{153}Sm-ZLD was prepared followed by *in vitro* and *in vivo* studies in wild-type rats up to 7 d and preliminary dose evaluation for human was performed based on biodistribution data in rats and by RaDAR method.

METHODS

The zoledronic acid was kindly provided by Faculty of chemistry, Khajeh Nasir Toosi University of Technology (Iran), and utilized without further purification. Samarium(III) nitrate hexahydrate was purchased as reagent-grade chemical from Sigma Aldrich Chemical Co and used without further purification. Infrared spectra were recorded using KBr disks with a Bruker vector 2 FT-IR instrument. Elemental analyses were performed on an Elementol vario-El CHN elemental analyzer. Absolute samarium and phosphorous percentages were determined by an Optima 7300VD atomic absorption-flame spectrometer. Thermogravimetric analysis (TGA & DSC) was carried out in the temperature range of 80 ~800 ºC at a heating rate of 6 ºC/min on a STA 1500 rheometric scientific instrument under nitrogen atmosphere.

Production of ^{153}Sm was performed at a research reactor using ^{152}Sm(n,γ)^{153}Sm nuclear reaction at Tehran Research Reactor (TRR). Samarium-152 with a purity of >98 % was obtained from ISOTEC Inc. Radio-chromatography was performed by counting of ITLC-SG and/or Whatman papers using a thin layer chromatography scanner, Bioscan AR2000, Paris, France. ITLC-SG was purchased from Agilent. UK. Other chemicals were purchased from Sigma-Aldrich. Analytical HPLC to determine the specific activity was performed by a Shimadzu LC-10AT, armed with two detector systems, flow scintillation analyser (Packard-150 TR) and UV–Visible (Shimadzu) using Whatman Partisphere C-18 column 250 x 4.6 mm (Whatman Co., NJ, USA). A high purity germanium (HPGe) detector coupled with a Canberra™ (model GC1020-7500SL) multichannel analyzer and a dose calibrator ISOMED 1010 (Dresden, Germany) were used for counting distributed activity in rat organs. Calculations were performed based on the 103 keV peak for ^{153}Sm.

Animal studies were performed in accordance with the United Kingdom Biological Council's Guidelines on the Use of Living Animals in Scientific Investigations, 2nd edn. The wild-type rats weighing between 180-200 g were acclimatized at proper rodent diet. RAdiation Dose Assessment Resource (RADAR) software was used for the calculation of the absorbed dose of each human organ based on biodistribution data in wild-type rats. The ligand and complexes were initially energy minimized at PM6 and PM6/SPARKLE. All calculations were carried out by means of MOPAC2012, the code developed by Dutra et al. [13] and for visualization Jmol and ChemCraft graphical softwares, were used [14, 15].

Synthesis and structural determination of Sm-ZLD complex

Samarium(III) nitrate hexahydrate (6 mmol, 22 mg) was dissolved in distilled water (5 mL), and an aqueous solution (5 mL) containing zoledronic acid (ZlH_2) (0.05 mmol, 13.6 mg) was added with stirring.

The pH of the resultant mixture was taken acidic by addition of few drops of hydrochloric acid and was stirred for 1h. Then, the resulting solution was filtered and left unperturbed to slowly concentrate. After three weeks, the colorless precipitate was collected by filtration and washed several times with distilled water.

The solid was almost insoluble in all common solvents. Yield: 45%; based on $Sm(NO_3)_3{\cdot}6H_2O$. Anal. calcd for $(C_{10}H_{31}N_4O_{21}SmP_4)_n$ (MW= 817.62 g $M^{-1})_n$: C, 14.69; H, 3.82, N, 6.85; P, 15.15; Sm,18.39. Found: C, 14.63; H, 3.41, N, 6.82; P, 15.11; Sm, 18.30%. Selected IR data (ν/cm^{-1}) 3144 (s), 1635 (w), 1581(m), 1545 (w), 1384 (s), 1309 (w), 1188 (s), 1152 (s), 1093 (m), 1066 (m), 961(m), 904 (m), 720 (w), 687 (w), 624 (m), 582 (m), 550 (s), 466 (m).

Production and quality control of $^{153}SmCl_3$ solution

Samarium-153 was produced by neutron irradiation of 100 µg of enriched $^{152}Sm_2O_3$ (^{152}Sm, 98.7 % from ISOTEC Inc.) according to reported procedure [14] by a research reactor at a thermal neutron flux of 5×10^{13} n cm^{-2} s^{-1} for 5 days. Specific activity of the produced ^{153}Sm was 819 mCi/mg. The irradiated target was dissolved in 200 µL of 1.0 M HCl, to prepare $^{153}SmCl_3$ and diluted to the appropriate volume with ultra-pure water, to produce a stock solution. The mixture was filtered through a 0.22-µm biological filter and sent for use in the radiolabelling step. The radionuclidic purity of the solution was tested for the presence of other radionuclides using beta spectroscopy as well as HPGe spectroscopy for the detection of various interfering beta and gamma emitting radionuclides. The radiochemical purity of the $^{153}SmCl_3$ was checked using 2 solvent systems for ITLC [A, 10 mM DTPA pH 5 and B, ammonium acetate 10 %: methanol (1:1)]. A, a mixture of 10 mM DTPA solution (pH 5) as the mobile phase on Whatman No. 2 paper, the free samarium cation in $^{153}Sm^{3+}$ form, was chelated with the polydentate eluting leading to the migration of the cation in ^{153}Sm- DTPA form to higher R_f (R_f 0.7), any other ionic species would lead to the observation of new radiopeaks, especially at the origin (R_f 0.0–0.1). B, a mixture of 10 % ammonium acetate:methanol (1:1) was used as another solvent system on the Whatman No. 2 paper, $^{153}Sm^{3+}$ remains at the origin using this system while other ionic species would migrate to higher R_fs. The radiochemical purity was higher than 99 %.

Preparation of ^{153}Sm-ZLD

A stock solution ZLD was prepared by dissolving 50 mg of the solid in 1 M NaOH (1 mL). For labelling, an appropriate amount of the $^{153}SmCl_3$ solution, containing the required activity was added to the desired amount of ZLD solution (0.2 mL).

The mixture was maintained at 40ºC for 2 hours followed by passing through a 0.22 µm membrane filter and the pH was adjusted to 7-8.5 with 0.05M phosphate buffer (pH = 5.5). The radiochemical purity was determined using Whatman chromatography paper, eluted with NH_4OH 18 M (56%): methanol: water (0.2:2:4; v/v/v) mixture. HPLC was performed with a flow rate of 1 mL/min, pressure: 130 kgF/cm2 for 20 min using a mixture of water:acetonitrile 3:2(v/v) as the eluent by means of reversed phase column Whatman Partisphere C_{18} (4.6 × 250 mm). The radiocomplex peak was consistent with the standard peak obtained by trace injection of the cold complex.

Stability studies

The stability of ^{153}Sm-ZLD stored at room temperature (25 ºC) at 2, 4, 8, 12 and 24 h after incubation (n=5) were checked by determining the radiochemical purity of the complex by paper chromatography in NH_4OH (18M) :MeOH:H_2O (2:20:40) system.

In vitro stability of ^{153}Sm-ZLD in presence of human serum

Final solution (200 µCi, 50 µL) was incubated in the presence of freshly prepared human serum (300 µL) (Purchased from Iranian Blood Transfusion Organization, Tehran) and kept at 37ºC for 2 h. Trichloroacetic acid (10%, 100µl) was added to a portion of the mixture (50 µl) every 30 min and the mixture was centrifuged at 3000 rpm for 5 min. The debris was decanted from the supernatant. The stability was determined by performing frequent ITLC analysis of supernatant using above mentioned ITLC system.

Hydroxyapatite binding assay

The hydroxyapatite binding (HA) assay was performed according to the procedure [15]. in 2002, with only a slight modification. In brief, to vials containing 1.0, 2.0, 5.0, 10.0, 20.0 and 50.0 mg of solid h HA, 2 ml of saline solution of pH 7.4 were added and the mixtures were shaken for 1h. Then, 50 µl of the radioactive preparation (containing 100-300µCi) was added and the mixtures were shaken for 24 h at room temperature. The suspensions were centrifuged, and two aliquots of the supernatant liquid were taken from each vial and the radioactivity was measured with a well-type counter. Test experiments were performed using a similar procedure, but in the absence of HA.

The percentage binding of ^{153}Sm-labeled compound to HA was calculated according to HB=1-A/B×100, where A is the mean radioactivity value of the supernatant sample under study and B is the mean total value of whole activity used.

Biodistribution of ^{153}Sm cation and ^{153}Sm-ZLD in wild-type rats

For biodistribution studies, 50-100 µl of $^{153}SmCl_3$ in acetate buffer pH. 5.5 and final ^{153}Sm-ZLD solution with 200 µCi radioactivity were injected intravenously to rats through their tail vein. The animals were euthenised at the exact time intervals (2, 4, 24, 48, 72 and 168 h) post injection the percent injected dose per gram (%ID/g) of different organs was calculated based on the measurements of HPGe detector. For each time interval 3 animals were used.

Dosimetric studies

The absorbed dose of each human organ was calculated by RaDAR method based on biodistribution data in wild-type rats. In this method, an electronic resource was established to obtain the tables of dose factors for use in internal dose assessment in nuclear medicine, radiation protection and other applications by RADAR group (eq.1).

$$D = N \times DF \quad (1)$$

Where N is the number of disintegrations that occur in a source organ, and DF represents the physical decay characteristics of the radionuclide, the range of the emitted radiations, and the organ size and configuration. In RaDAR method, DFs were derived using Monte Carlo simulation of radiation transport in models of the body and its internal structures by the latest versions of human phantoms and are calculated as eq.2:

$$DF = \frac{k \sum_i n_i E_i \phi_i}{m} \quad (2)$$

Where n_i is the number of radiations with energy E emitted per nuclear transition, E_i is the energy per radiation (MeV), ϕ_i is the fraction of energy emitted that is absorbed in the target, m is the mass of target region (kg) and k is some proportionality constant ($\frac{mGy.kg}{MBq.s.MeV}$). DFs are constant values for a specified radionuclide and are tabulated for any source to target organ. In this study, DFs have been taken from the OLINDA/EXM software [16].

Since the biodistribution studies were performed in animals, the accumulated activity in animals should be extrapolated to the accumulated activity in humans. This extrapolation was carried out by the proposed method of Sparks et al. [17] (eq.3).

$$N_{human\ organ} = N_{animal\ organ} \frac{Organ\ Mass_{human} / Body\ Mass_{human}}{Organ\ Mass_{animal} / Body\ Mass_{animal}} \quad (3)$$

Where N is the accumulated activity in the source organs and can be calculated by plotting the percentage-injected dose versus time for each organ and computing the area under the curves (eq.4).

$$N = \int_{t_1}^{\infty} N(t)\, dt \quad (4)$$

Where N (t) is the activity of each organ at time t. In order to calculate N, the data points representing the percentage-injected dose were created and linear approximation between the two experimental points of times were used. The curves were extrapolated to infinity by fitting the tail of each curve to a mono-exponential curve with the exponential coefficient equal to physical decay constant of ^{153}Sm. For extrapolation the accumulated activity to human, the mean weights of each organ for standard human were used according to OLINDA code 2007.

RESULTS AND DISCUSSION

Synthesis and structural determination of Sm-ZLD complex

The compound was prepared by one-pot reaction and almost insoluble in all common solvents. Formation of the samarium(III) complex can be established from elemental analysis, IR spectroscopy and thermogrametic data. These results showed that the compound contains zolderonic acid, samarium ion and water molecules in mole ratios of 2:1:7, respectively. Attempts to obtain single crystals of the compound have been failed so far. The IR spectrum of the free ligand has indicator bands that are apparent with minor shift in the complex. Presence of a broad structureless band at around 3140 cm^{-1} in the complex can be assigned to the O-H stretching frequency of the water molecule. Dependence on coordination is also exhibited by intense bands occurring at 1188 and 1151 cm^{-1} which is associated with P=O vibration and are observed at higher frequencies (1288 and 1263 cm^{-1}) and less intense in the free zolderonic acid. The presence of the P-O group in the complex was also declared by a medium band at around 1066 cm^{-1} and which are attributed to the anti-symmetric stretching vibration mode. This vibrational band occurs in 1093 cm^{-1} in free ligand. At lower frequency the complex also exhibited a medium band 466 cm^{-1} which is attributed to the ν(Sm-O) vibration mode (Table 1).

Table 1: the major band peaks in infrared spectroscopy of ZLD (ligand) and ^{153}Sm-ZLD (complex).

Ligand (cm^{-1})	Complex (cm^{-1})	Chemical bond
1288	1188	P=O
1263	1151	P=O
1182	1118	P-O
1093	1065	P-O
976	961	P-O
919	904	P-O

The strong bands at 1182 and 1093 $cm^{-1}$are related to unsymmetrical stretching vibrations for P-O bonds and 919 and 961 cm^{-1} are related for symmetrical vibrations. In the complex, all the bands showed blue-shift as a result of metal-ligand interaction Broad bands in the range of 3200-3400Cm^{-1} demonstrates the existence of water molecule in the complex structure while not observed in the ligand spectrum. Also bands observed in the range of 3000-3200 cm-1 correspond to the N-H stretching vibrations on the imidazole ring in zoledronic structure as observed by Qiu et al, and also in other metal-ZLD complexes reported [18].

The thermal analysis of the compound was evaluated by thermogravimetric analysis (TG and DSC) which explores its thermal stability. TG curve indicates the weight loss of 15.6% from 50 to 150 °C that can be ascribed to the removal of seven water molecules [15.4% calcd. based on $Sm(ZL)_2.7H_2O$)]. Thus, during the heating**,** it was lost with an endothermic associated process (Figure 1).

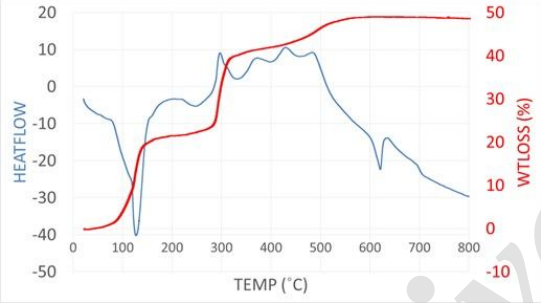

Fig 1. TGA and DSC curves for Sm–ZLD compound.

The next weight loss is apparent between 270 and 315 °C and can be attributed to the loss of two pyrazyl moieties (HO–CH_2-Pyz) corresponding to 39.2% of the weight loss (calculated 39.1%). The compound further started to decomposition at 350 °C and finished at ca. 600 °C due to burn out of the rest of the organic part of the compound.

Theoretical modeling of the complexation

In order to discover more information on the structural features and thermochemistry of Sm/zelodronate complexes, the following simplified reactions were considered for theoretical studies:

$$[Sm(OH_2)_9]^{+3} + L^{-2} \longrightarrow [SmL(OH_2)_5]^{+} + 4H_2O \quad (R1)$$

$$[SmL(OH_2)_5]^{+} + L^{-2} \longrightarrow [SmL_2(\bar{H}_2O)_3]^{-} + 2H_2O \quad (R2)$$

$$[SmL_2(\bar{H}_2O)_3]^{-} + L^{-2} \longrightarrow [SmL_3]^{-3} + 3H_2O \quad (R3)$$

where the symbol " L " denotes to zelodronate ligand. The reactions R_1, R_2 and R_3 refer to the formation of 1:1, 1:2 and 1:3 complexes (SmL, SmL_2 and SmL_3). Zelodronate is a polyprotic acid having four ionizable P-OH groups and one amino ($-NH_2$) group. Successive deprotonation of this pentaprotic acid (referred to as H_5L) results in other protonation states of ZLD. In this study we have focused our modeling on that state which is relevant to the preparation of ligand solution at pH=8 (that is H_3L).

As the first coordination sphere of lanthanides ion in solution usually is fully saturated with solvent molecules, the solvated geometry of Sm^{+3} was considered to be $[Sm(OH_2)_9]^{+3}$ which is the most common structure of lanthanide ions in aqueous media. Among the various quantum mechanical approaches, PM6 method was used for geometry optimization and thermochemistry analysis of the R1-R3 reactions. As reported earler by Dutra et al. [13], it should be noted that PM6 is one the most recent member of the NDDO family of semi-empirical methods and is understandably the most accurate. This method has been fully parameterized to reproduce geometry and enthalpy of formation of a variety of organic molecules. The PM6/SPARKLE method was applied for many reactions reported by Anderade et al. In the parameterization of the sparkle model for the lanthanide complexes, 4f orbitals are contracted towards the ion by the outermost 5s and 5p closed shells and the lanthanide ion was represented by SPARKLE. This method is known as a reliable model to predict the geometry of lanthanide complexes. The accuracy of this method is competitive with the ab initio/effective core potential calculations especially for the large-size lanthanide complexes, while the former being hundreds of times faster as seen by Cao [19, 20]. The optimized geometry of ligand at PM6 level is represented in Figure 2. For the aim of compassion selective geometrical parameters of free ligand at AM1, PM6 and PM7 level of theory together with available experimental values are reported in Table 2.

The obtained results reveal that the average P-O bond lengths in P-OH group is about 0.15A longer than same parameter in P-O moiety. A comparison between calculated and experimental results shows that PM6 is a proper method for reproducing geometrical parameters of the system. For example the reported experimental value for P-C-P angle is 116.4 while the calculated values at AM1 and PM7 are 137.9 and 112.4, respectively. Moreover there is good agreement between calculated bond lengths and those of experimental values. One may conclude that PM6 method provides the closest values of geometrical parameters to those of experimental values, therefore this method in conjugation of SPARKLE model (denoted as PM6/SPARKLE) is selected for geometry optimizations of complexes.

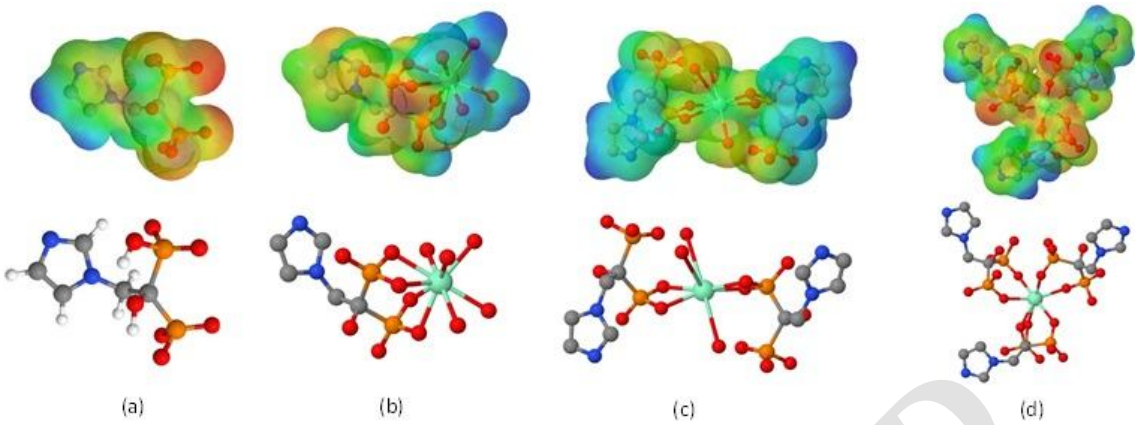

Fig 2. Schematic representation of optimized geometries and corresponding electrostatic potential energy maps of: (a) deprotonated ZLD ligand, (b) Sm(ZLD), (c) $Sm(ZLD)_2$ and (d) $Sm(ZLD)_3$.

In Figure 2a, schematic representation of electrostatic potential energy map of deprotonated ligand (L-2) is shown. These maps which illustrate the charge distributions of molecules three dimensionally allow us to visualize variably charged regions of a molecule. Knowledge of the charge distributions can be used to determine how molecules interact with one another. In this figure the red color corresponded to the lowest electrostatic potential energy, the blue indicates the highest electrostatic potential energy and intermediary colors represent intermediary electrostatic potentials. There is a reverse relationship between electrostatic potential and charge distribution. Low potential, red, are considered by a great quantity of electrons and high potential, blue, are characterized by a relative lack of electrons. Oxygen atoms have a higher electronegativity value and charge density than phosphorus atoms leading to a higher electron density around them. Thus these sites may involve in the interaction with Sm^{+3} cation. The similar electrostatic potential energy maps of SmL, SmL_2 and SmL_3 are shown in Figures 2b-2d.

Table 2: Selected geometrical parameters of zelodronate ligand at various semi-empirical computational levels. Bond lengths are in angstrom and the angle is in degree.

Bond/Angle	AM1	PM6	PM7	Exp.
P-OH	1.60	1.63	1.60	1.64
P-O	1.45	1.48	1.46	1.47
P-C	1.75	1.90	1.95	1.89
P-C-P	137.90	116.60	122.10	116.40

As it is expected the complexation procedure effects on ligand geometry leading to ligand deformation. The average P-O bond lengths are increased from 1.51A in free ligand to 1.55A, 1.54A and 1.55A in SmL, SmL_2 and SmL_3, respectively. In the other words the complexation has weakened the initial P-O bonds by increasing the average bond lengths. The backbone angle (that is P-C-P angle) decreased during complexation which may be related to increasing overlap between oxygen atoms orbitals and unoccupied orbitals of metal ion.

It is seen that due to steric repulsions between ligands and aqua molecules not only the coordination number of Sm^{+3} has decreased from CN=9 to CN=7, but also the average distance of coordinated aqua are increased. In other words, due to steric effect of high electron density ZLD ligands, no water molecule could be left in the first coordination sphere of the complex.

Table 3 presents the calculated momentdipole (μ), enthalpy of formation (ΔHf), total energy (Et) and HOMO-LUMO energy gap for all studied complexes. The enthalpy and energy changes for reactions R1 to R3 at 298ºK are also reported. The calculated dipole moment for SmL, SmL2 and SmL3 are 9.4D, 3.2D and 4.0D, respectively. Considering the dominant dipole-dipole interaction as one of the main effective factors in solubility, one may predict higher solubility for SmL compare to SmL_2 and SmL_3 that is higher hydrophilicity of SmL than the other complexes. Moreover, the value of enthalpy of formation and total energy may be considered as a measure of system stability. The data in Table 3 suggest the following order of stability for studied complexes: SmL_3>SmL_2>SmL. The complexation reactions lead to decrease HOMO-LUMO energy gap from 15.79 ev in $[Sm(H_2O)_9]^{3+}$ to average value of 9.6ev in complexes. The close values of HOMO-LUMO energy gap, suggest analogous electronic absorption spectra for these complexes.

Table 3: Thermochemistry data of R1-R3 reactions.

System	μ(D)	ΔH_f(kcal/mol)	E_t(au)	ΔH_r(kcal/mol)	ΔE_r(kcal/mol)	Gap(ev)
$[SmL(H_2O)_5]^{+1}$	9.5	-575.8	-5045.5	-487.1	-21.1	9.301
$[SmL_2(H_2O)_3]^{-1}$	3.2	-1026.7	-7826.2	-145.7	-6.3	9.922
$[SmL_3]^{-3}$	4.0	-1371.2	-10285.7	-93.7	953.2	9.649
$[Sm(H_2O)_9]^{+3}$	1.0	107.8	-2888.1	-	-	15.793

The enthalpy and energy changes suggest that all reactions (R_1-R_3) are exothermic. As the change in entropy (ΔS) for these type of reactions are positive, one may conclude that the changes in Gibbs' free energy (ΔG) of formation at temperature of T are negative (due to $\Delta G = \Delta H - T\Delta S$). The change in Gibbs' free energy associated with a chemical reaction is a useful indicator of whether the process will proceed spontaneously. A negative ΔG associated with a reaction indicates that it can happen spontaneously. Thus the formation of aforementioned complexes is carried on spontaneously. It is expected that these thermochemistry results together with geometrical features will provide useful information for designing new force fields required to perform molecular dynamics simulations (MD) on Sm/ZLD radiopharmaceutical.

Radionuclide production

The radionuclide was prepared in a research reactor with a range of specific activity between 3 to 5 GBq/mg for radiolabelling use. After counting the samples on an HPGe detector for 5 min, two major photons (70.68 keV and 103 keV)_were observed. Radionuclidic purity was higher than 99.96 %. The radiochemical purity of the $^{153}SmCl_3$ was checked using two solvent systems for ITLC (A: 10 mM DTPA pH 4 and B: ammonium acetate 10% :methanol (1:1; v:v).

Radiolabeling of ZLD with $^{153}SmCl_3$

In order to obtain maximum complexation yield, several experiments were carried out by varying different reaction parameters such as ligand:Sm ratio, pH, and reaction time. The radiochemical purity of more than 99% was achieved at pH 7-8 and 40-50ºC with 50:1 ligand molar ratio to calculated samarium content. The reaction mixture was incubated at room temperature AND 50ºC for different time periods and 120 min incubation was found to be adequate to yield maximum complexation. The best ITLC mobile phase was considered Whatman paper using NH_4OH (18M): MeOH: H_2O (0.2:2:4). In the chromatographic system of choice, free samarium cation elutes to the R_f of 0.1 while the radiolabeled bisphosphonate complex migrates to higher Rf_s, i.e. 0.9 (Figure 3).

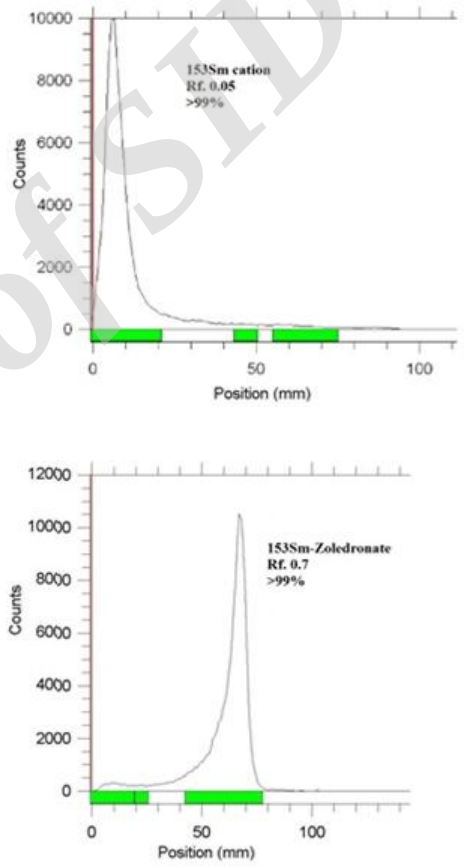

Fig 3. ITLC radiochromatograms for ^{153}Sm solution (above) and ^{153}Sm–ZLD (below) using NH4OH:MeOH:H2O (0.2:2:4) on Whatman 3 MM.

Variations in complexation yields with respect to the ZLD:samarium molar ratio is shown in Table 4. At pH 7-8 and 40°C the best saturated molar ratio was observed for 50:1 ratio, while a major drop in radiochemical purity is observed in reducing 40 to 20. At the optimized conditions specific activity of 4.4 GBq/mmol was obtained.

Table 4. Complexation yields of ^{153}Sm-ZLD at different ligand:metal ratios.

Sm:ZLD molar ratio	Radiochemical yield (%)
01:05	46 ± 0.5
01:10	50± 0.6
01:15	59 ± 0.2
01:20	73 ± 0.3
01:40	97 ± 0.4
01:50	99± 0.4

In HPLC experiments using a mixture of water:acetonitrile would lead to the fast removal of any free cation from the column with a retention time of 1-1.5 min starting from water, while with increasing the amount of acetonitrile content in the mobile phase mixture the radiolabelled complex is washed out (7-7.3 min) (Figure 4).

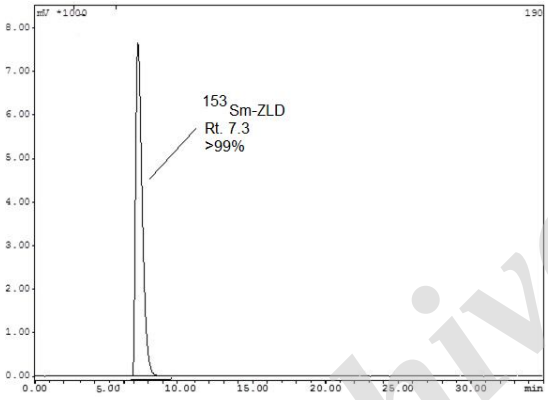

Fig 4. HPLC chromatogram of ^{153}Sm–ZLD final solution on a reversed phase column using acetonitrile:water 40:60, up; using scintillation detector

Stability studies

The stability of the complex prepared under optimized reaction conditions was studied at room temperature and in presence of human serum at 37°C. It was observed that the complex was >95% stable both at room temperature and in presence of human serum at 37ºC even after 24 h.

Hydroxyapatite assay

The assay demonstrated high capacity binding for ^{153}Sm-ZLD to hydroxyapatite. Even at 3 mg amount of HA, about 80% binding was observed, while at 5 mg HA used >95% of binding was obtained. Compared to the other radiolanthanide ZLD complex, *i.e.*, ^{177}Lu-ZLD, the samarium complex demonstrates higher hydroxyapatite binding, while Sm complex reaches the 90% affinity at 15 mg of hydroxyapatite (Figure 5).

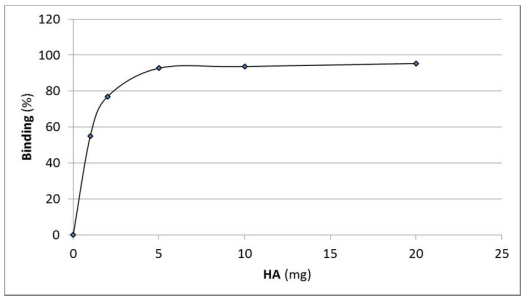

Fig 5. The HA binding assay data for ^{153}Sm-ZLD

Biodistribution of ^{153}Sm-cation and ^{153}Sm-ZLD in wild-type rats

For ^{153}Sm cation, as reported earlier [21], the biodistribution was mainly accumulated in the liver, kidney and bone.

As it can be seen in Figure 5, the major portion of the injected activity of ^{153}Sm-ZLD was accumulated in bones as expected for bone-avid radiopharmaceuticals. ^{153}Sm-ZLD is rapidly uptake in bones in 2 h after administration and increases up to 48 h (14%). ^{153}Sm-ZLD has low liver, spleen, stomach and lung accumulation (<1 %), which is a major advantage as a therapeutic radiopharmaceutical for possible human use, not exceeding the maximum allowed administered dose to liver. Interestingly the renal uptake of the agent is much higher than other ^{153}Sm-bisphosphonates, an effect that has not been observed in the agents studied other than ZLDs, reaching to more than 9% in 4h (Figure 6).

This observation can be explained by a very recent report by researchers using a primary human tubular cell culture system, using double labeled zoledronic acid (fluorescently/radiolabeled) concluding that fluid-phase-endocytosis of zoledronic acid and cellular accumulation at high doses may be responsible for high ZLD renal uptake as reported earlier [22]. Thus the high renal uptake of the complex in this study is not only explained by renal excretion but also by fluid-phase-endocytosis.

The recent biodistribution data for ^{153}Sm-EDTMP as the most important bone pain palliation therapy agent [23] and also recently developed candidate complex, ^{153}Sm-BPAMD [24], show target:non target ratios comparable to the developed complex in this study as presented in Tables 5 and 6.

Bone/non-target ratios for ^{153}Sm-ZLD at different time intervals has been demonstrated in Table 7.

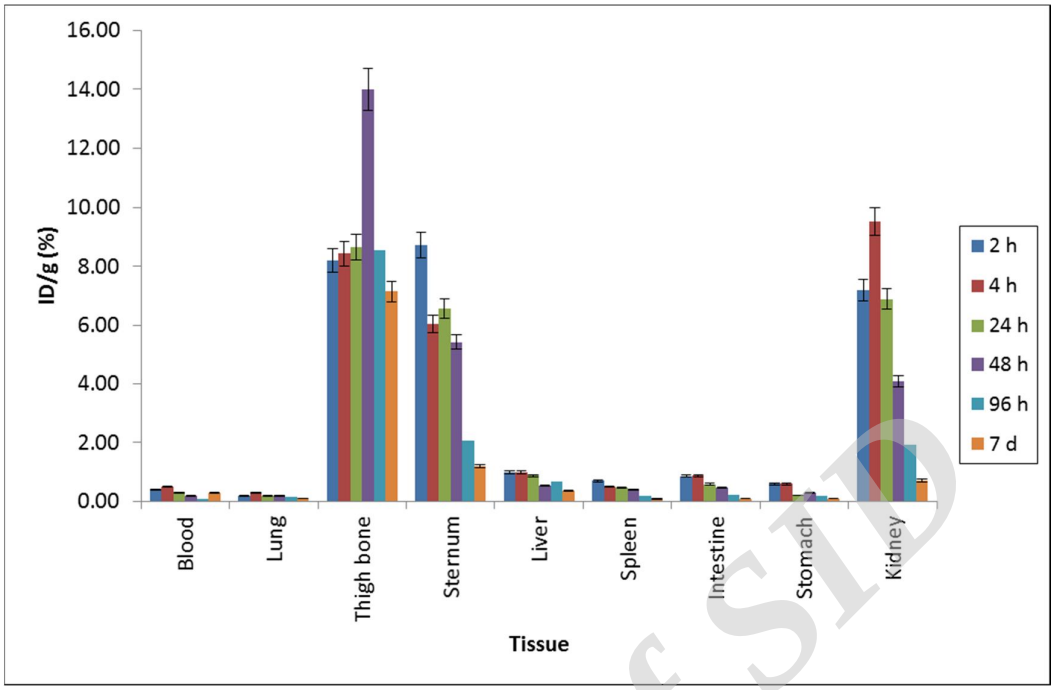

Fig 6. Percentage of injected dose per gram of ^{153}Sm-ZLD in wild-type rat tissue after 2, 4, 24, 48, 96 h and 7 days post injection.

Table 5: Bone/non-target ratios for ^{153}Sm-EDTMP at different time intervals [21].

Bone/non-target ratios	2h	4h	24 h	48 h
bone:liver	22.34	20.16	16.45	17.72
bone:kidney	6.74	11.02	17.93	16.76

Table 6: Bone/non-target ratios for ^{153}Sm-BPAMD at different time intervals [13].

Bone/non-target ratios	2 h	4 h	24 h	48 h
bone:liver	17.38	24.28	17.82	32.13
bone:kidney	5.48	11.94	15.53	18.63

Table 7. Bone/non-target ratios for ^{153}Sm-ZLD at different time intervals.

Bone/non-target ratios	2 h	4 h	24 h	48 h
bone:liver	8.20	8.43	9.94	25.92
bone:kidney	1.14	0.89	1.25	4.44

Dosimetric studies

Dosimetric evaluation in human organs was performed by RADAR method based on biodistribution data in rat organs. The absorbed dose in each human organ after injection of ^{153}Sm-ZLD is given in Figure 7. In this work, ^{153}Sm-ZLD was produced as a bone pain palliative agent and its biodistribution was studied up to 48 h post injection. As it can be seen in Figure 7, significant bone uptake was observed 2 h post injection, whereas accumulation in vital organs was negligible.

Due to the direct relationship between absorbed dose and response in terms of cell killing/survival, calculation of the radiation absorbed dose to a targeted tissue is an important parameter which should be considered [25]. In this study, the absorbed dose to each human organ was investigated based on biodistribution data in rats and by RaDAR method and compared with the absorbed dose in each human organ for ^{153}Sm-ZLD. The highest absorbed dose for ^{153}Sm-ZLD is observed in osteogenic cells and kidneys with 0.28 and 0.26 mSv/MBq respectively.

CONCLUSION

^{153}Sm-ZLD complex was prepared in high radiochemical purity (>99%, ITLC, HPLC) and specific activity of 4.4 GBq/mmol. The complex demonstrated significant stability at room temperature and in presence of human serum at 37◦C even after 24 h. Complex binding to hydroxyapatite (5 mg) was >95%.

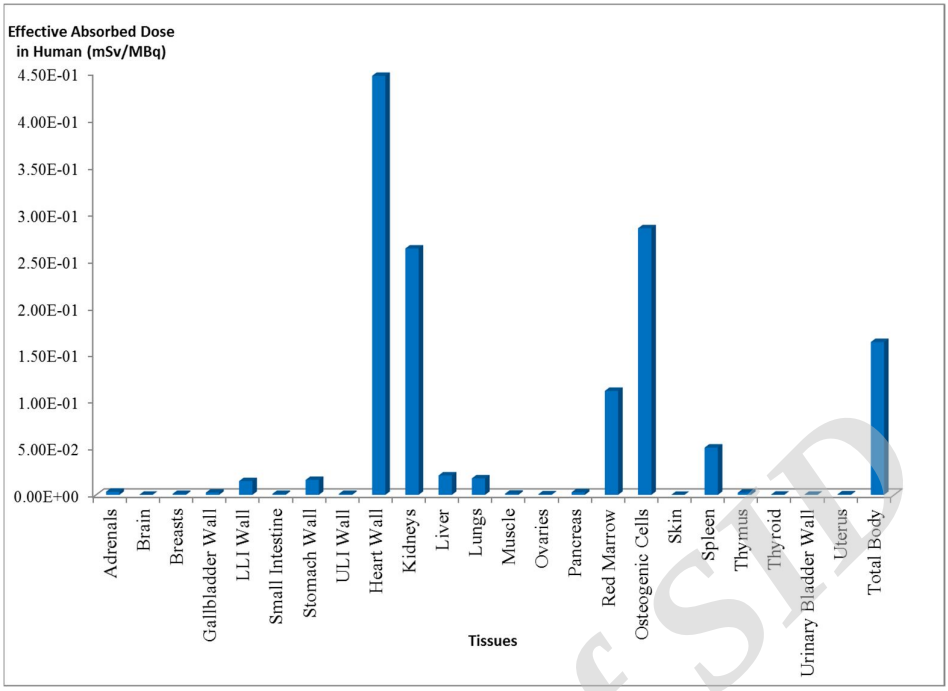

Fig 7. The calculated absorbed dose in each human organ after injection of ^{153}Sm-ZLD.

Theoretical investigations not only showed the formation of metal/ ligand complexes but also suggests that the formation of aforementioned complexes will proceed spontaneously.The major accumulation of the radio-complex was in the bone and kidneys. Absorbed dose evaluation of these organs by RaDAR software for kidneys and osteogenic tissues were 0.26 and 0.28 mSv/MBq; respectively. ^{153}Sm-ZLD demonstrated significant bone uptake comparable to clinically applied ^{153}Sm-radiopharmaceuticals.

REFERENCES

1. Palma E, Correia JD, Campello MP, Santos I. Bisphosphonates as radionuclide carriers for imaging or systemic therapy. Mol Biosyst. 2011 Nov;7(11):2950-66.
2. Fleisch H, Russell RG, Francis MD. Diphosphonates inhibit hydroxyapatite dissolution in vitro and bone resorption in tissue culture and in vivo. Science. 1969 Sep 19;165(3899):1262-4.
3. Majkowska A, Neves M, Antunes I, Bilewicz A. Complexes of low energy beta emitters 47Sc and 177Lu with zoledronic acid for bone pain therapy. Appl Radiat Isot. 2009 Jan;67(1):11-3..
4. Abruzzese E, Iuliano F, Trawinska MM, Di Maio M.153Sm: its use in multiple myeloma and report of a clinical experience. Expert Opin Investig Drugs. 2008 Sep;17(9):1379-87.
5. D'angelo G, Sciuto R, Salvatori M, Sperduti I, Mantini G, Maini CL, Mariani G. Targeted "bone-seeking" radiopharmaceuticals for palliative treatment of bone metastases: a systematic review and meta-analysis. Q J Nucl Med Mol Imaging. 2012 Dec;56(6):538-43.
6. Simón J, Frank RK, Crump DK, Erwin WD, Ueno NT, Wendt RE 3rd. A preclinical investigation of the saturation and dosimetry of 153Sm-DOTMP as a bone-seeking radiopharmaceutical. Nucl Med Biol. 2012 Aug;39(6):770-6.
7. Astrand J, Aspenberg P. Topical, single dose bisphosphonate treatment reduced bone resorption in a rat model for prosthetic loosening. J Orthop Res. 2004 Mar;22(2):244-9.
8. http://www.cancerresearchuk.org/about-cancer/cancers-in-general/treatment/cancer-drugs/zoledronic-acid (viewed Nov. 23, 2015)
9. Asikoglu M, Durak FG. The rabbit biodistribution of a therapeutic dose of zoledronic acid labeled with Tc-99m. Appl Radiat Isot. 2009 Sep;67(9):1616-21.
10. Qiu L , Lin J, Cheng W, Wang Y, Luo S. 99mTc-labeled butyl-substituted zoledronic acid as a novel potential SPECT imaging agent: preparation and preclinical pharmacology study. Med Chem Res. 2013;22(12):6154-6162.
11. Nikzad M, Jalilian AR, Shirvani-Arani S, Bahrami-Samani A, Golchoubian H. Production, quality control and pharmacokinetic studies of 177Lu-Zoledronate for bone pain palliation therapy. J Radioanal Nucl Chem. 2013;298:1273–1281.
12. Arabieh M. Khodabandeh MH, Karimi-Jafari MH, Platas-Iglesias C. Zare K. Complexation of Sm3+ and pamidronate: A DFT study. J Rare Earths. 2015;33(3):310–319.
13. Dutra JD1, Filho MA, Rocha GB, Freire RO, Simas AM, Stewart JJ. Sparkle/PM7 Lanthanide Parameters for the

Modeling of Complexes and Materials. J Chem Theory Comput. 2013 Aug 13;9(8):3333-3341.

14. International Atomic Energy Agency. Manual for reactor produced radioisotopes. Vienna: IAEA; 2003. p.189-192.

15. Neves M, Gano L, Pereira N, Costa MC, Costa MR, Chandia M, Rosado M, Fausto R. Synthesis, characterization and biodistribution of bisphosphonates Sm-153 complexes: correlation with molecular modeling interaction studies. Nucl Med Biol. 2002 Apr;29(3):329-38.

16. OLINDA - Organ Level Internal Dose Assessment Code (Version 1.1), 2007. copyright Vanderbilt University.

17. Sparks RB, Aydogan B. Comparison of the effectiveness of some common animal data scaling techniques in estimating human radiation dose. Sixth International Radiopharmaceutical Dosimetry Symposium. Oak Ridge, TN: Oak Ridge Associated Universities; 1996. p. 705-16.

18. Qiu L, Lin J, Wang L, Cheng W, Cao Y, Liu X, Luo S. A Series of imidazolyl-containing bisphosphonates with abundant hydrogen-bonding interactions: syntheses, structures, and bone-binding affinity. Aust J Chem. 2014;67(2):192-205.

19. Cao DK, Li YZ, Zheng LM. Layered cobalt(II) and nickel(II) diphosphonates showing canted antiferromagnetism and slow relaxation behavior. Inorg Chem. 2007 Sep 3;46(18):7571-8.

20. Cao DK, Liu MJ, Huang J, Bao SS, Zheng LM. Cobalt and manganese diphosphonates with one-, two-, and three-dimensional structures and field-induced magnetic transitions. Inorg Chem. 2011 Mar 21;50(6):2278-87.

21. Naseri Z, Hakimi A, Jalilian AR, Shirvani-Arani S, Bahrami-Samani A, Ghannadi-Maragheh M. Synthesis, quality control and biological evaluation of tris[(1,10-phenanthroline)[153Sm]samarium(III)]trithiocyanate complex as a therapeutic agent. Radiochim Acta. 2012;100(4):267-272.

22. Verhulst A, Sun S, McKenna CE, D'Haese PC. Endocytotic uptake of zoledronic acid by tubular cells may explain its renal effects in cancer patients receiving high doses of the compound. PLoS One. 2015 Mar 10;10(3):e0121861.

23. Bahrami-Samani A, Ghannadi-Maragheh M, Jalilian AR, Meftahi M, Shirvani-Arani S, Moradkhani S. Production, quality control and biological evaluation of 153Sm-EDTMP in wild-type rodents. Iran J Nucl Med. 2009;17(2):12-19

24. Rabie A, Enayati R, Yousefnia H, Jalilian AR, Shamsaei M, Zolghadri S, Bahrami-Samani A, Hosntalab M. Preparation, quality control and biodistribution assessment of ^{153}Sm-BPAMD as a novel agent for bone pain palliation therapy. Ann Nucl Med. 2015 Dec;29(10):870-6.

25. Talwer GP, Srivastava LM. Textbook of biochemistry and human biology. August 2004 Verlag: Prentice-Hall of India Pvt. Ltd. 2004.